

PD-1^{IR2} promotes tumor evasion via deregulating CD8⁺ T cell function

Haojing Zang ^{1,2} Tongfeng Liu,^{3,4} Xiaodong Wang,^{3,5} Shuwen Cheng,^{3,6} Xiaofeng Zhu,^{3,4} Chang Huang,^{3,4} Liqiang Duan,^{2,3} Xujie Zhao,³ Fang Guo,^{3,7} Xuotong Wang,^{3,5} Chang Zhang,^{3,8} Facai Yang,³ Yinmin Gu ^{9,10} Hongbo Hu,¹¹ Shan Gao ^{1,3}

To cite: Zang H, Liu T, Wang X, et al. PD-1^{IR2} promotes tumor evasion via deregulating CD8⁺ T cell function. *Journal for ImmunoTherapy of Cancer* 2025;13:e010529. doi:10.1136/jitc-2024-010529

► Additional supplemental material is published online only. To view, please visit the journal online (<https://doi.org/10.1136/jitc-2024-010529>).

Accepted 22 February 2025

ABSTRACT

Background The programmed cell death 1 (PD-1) is an immune checkpoint that mediates immune evasion of tumors. Alternative splicing (AS) such as intron retention (IR) plays a crucial role in the immune-related gene processing and its function. However, it is not clear whether *PDCD1* encoding PD-1 exists as an IR splicing isoform and what underlying function of such isoform plays in tumor evasion.

Methods An AS isoform of human *PDCD1*, characterized by the second IR and named PD-1^{IR2}, was identified by reverse transcription-PCR (RT-PCR) and Sanger sequencing. The expression profile of PD-1^{IR2} was assessed by quantitative RT-PCR and flow cytometry, while its function was evaluated through immune cell proliferation, cytokine interleukin 2 secretion, and tumor cell killing assays. *PDCD1*^{IR2 CKJ} mice which specifically conditional knock-in *PDCD1*^{IR2} in T cells and humanized peripheral blood mononuclear cells (PBMC)-NOG (NOD.Cg-PrkdcscidIL2rgtm1Sug/JicCrI) mice were utilized to further confirm the physiological function of PD-1^{IR2} in vivo.

Results PD-1^{IR2} is expressed in a variety of human leukemia cell lines and tumor-infiltrating lymphocytes. PD-1^{IR2} expression is induced on T cell activation and regulated by the RNA-binding protein hnRNPL. PD-1^{IR2} negatively regulates the immune function of CD8⁺ T cells, indicated by inhibiting T cell proliferation, cytokine production, and tumor cell killing in vitro. PD-1^{IR2} CD8⁺ T cells show impaired antitumor function, which consequently promote tumor evasion in a conditional knock-in mouse model and a PBMC-engrafted humanized NOG mouse model. PD-1^{IR2} mice exhibit resistance to anti-PD-L1 therapy compared with wild-type mice.

Conclusions PD-1^{IR2} is a potential immune checkpoint that may mediate potential resistance to immune checkpoint therapy.

INTRODUCTION

Immune checkpoints (ICs) are a class of immunosuppressive molecules that are expressed on immune cells and suppress immune cell activation.^{1,2} Programmed cell death 1 (PD-1) is one of the ICs, which negatively regulates T cell function by interacting with two ligands, PD-1 ligand 1 (PD-L1) and PD-L2.^{3,4} In addition, either PD-L1 or PD-L2 expressed by cancer cells binds to PD-1 on

WHAT IS ALREADY KNOWN ON THIS TOPIC

⇒ Alternative splicing (AS) is involved in the regulation of programmed cell death 1 (PD-1). Prior studies have shown that the isoforms of PD-1, such as Δ42 PD-1 and PD-1Δex3, play a crucial role in tumor immunity. However, whether PD-1 exists as an intron retention (IR) splicing isoform and what underlying function of such isoform plays remain to be further elucidated.

WHAT THIS STUDY ADDS

⇒ This study identified a new isoform, named as PD-1^{IR2}, which is expressed in a variety of human leukemia cell lines and tumor-infiltrating lymphocytes, and is regulated by hnRNPL. PD-1^{IR2} mediates tumor immune evasion and resistance to anti-PD-L1 antibody via deregulating CD8⁺ T cell function.

HOW THIS STUDY MIGHT AFFECT RESEARCH, PRACTICE OR POLICY

⇒ This study provides a new potential immune checkpoint and new insights into the resistance to clinical immune checkpoint blockade therapy. This will pave the way for developing small molecules targeting the IgV domain for both PD-1 and PD-1^{IR2}.

the surface of T cells, thereby inhibiting T cell activation and leading to cancer immune evasion.⁵ However, targeting PD-1/PD-L1 for patients with cancer has achieved some clinical benefits in a small subpopulation⁶; the underlying mechanism of such low response is imperative to be explored.

Alternative splicing (AS) refers to the process of producing various mRNA splicing isoforms from pre-mRNA,⁷ and contributes to proteomic diversity as well as regulates highly diverse processes, such as physiology or pathology, including cancer.⁷ AS is also involved in the regulation of ICs, such as Cytotoxic T lymphocyte antigen (CTLA)-4,^{8–10} PD-1^{11–14} and PD-L1.^{15,16} PD-1 AS isoforms include PD-1Δex3¹⁷, Δ42 PD-1¹¹ and PD-1^{Δ28}¹⁸; however, their molecular functions have not been well explained. As a major



© Author(s) (or their employer(s)) 2025. Re-use permitted under CC BY-NC. No commercial re-use. See rights and permissions. Published by BMJ Group.

For numbered affiliations see end of article.

Correspondence to

Dr Shan Gao; gaos@sibet.ac.cn

Dr Hongbo Hu;
hongbohu@scu.edu.cn

Dr Yinmin Gu;
guym_81@126.com

form of AS, intron retention (IR) regulates gene expression during CD4⁺ T cell activation.^{19–23} Nevertheless, whether the PD-1 IR isoform exists remains unknown. In our study, we identify a novel isoform of PD-1 with second IR termed as PD-1^{IR2}, which inhibits function of CD8⁺ T cells, thus promoting tumor evasion and being resistant to immunotherapy targeting PD-1/PD-L1. Our study reveals that PD-1^{IR2} may serve as a new IC and an underlying mechanism for resistance to immunotherapy.

RESULTS

The identification and regulation of PD-1^{IR2}

In our effort to amplify *PDCD1* transcript using reverse transcription-PCR (RT-PCR), we found a larger size band above wild-type (WT) *PDCD1*, which was verified as second IR isoform based on Sanger sequencing in the isolated peripheral blood mononuclear cells (PBMCs) (figure 1A and online supplemental figure 1A–C). PD-1^{IR2} contains signal peptide, IgV domain, and a new and short cytoplasmic tail (figure 1B and online supplemental figure 1D,E). To validate the presence of *PDCD1*^{IR2}, we further examined multiple human leukemia cell lines by PCR, which showed that *PDCD1*^{IR2} were expressed in certain cell lines (online supplemental figure 1F). Moreover, quantitative RT-PCR (qRT-PCR) assay with *PDCD1*^{IR2} specific primers revealed that *PDCD1*^{IR2} were expressed in these human leukemia cell lines, especially relatively high in Jurkat cell (figure 1C and online supplemental figure 1G). Collectively, our findings reveal that *PDCD1* has a second IR isoform at transcriptional level.

To specifically verify endogenous authentic PD-1^{IR2}, we used distinct 10 amino acid fragments from PD-1^{IR2} cytoplasmic tail as an antigen to generate antibodies, and obtained one monoclonal antibody that could specifically recognize PD-1^{IR2} by flow cytometry (FACS) in HEK293T cells overexpressing PD-1^{IR2} (online supplemental figure 1H). Furthermore, we verified this antibody specificity in endogenous PD-1^{IR2} levels in PHA-stimulated WT Jurkat cells and one *PDCD1*-knockout (KO) Jurkat cell line previously established by our lab¹⁸ (figure 1D). We overexpressed *PDCD1* and *PDCD1*^{IR2} in Jurkat KO-1 cells, respectively (online supplemental figure 1I), and western blot showed that PD-1^{IR2} mainly located intracellularly of Jurkat KO-1¹⁸ cells overexpressing PD-1^{IR2}, while it was almost undetectable in supernatant (online supplemental figure 1J), although PD-1^{IR2} lacks transmembrane domain. We wondered whether PD-1^{IR2} might be potentially induced on T cell activation in a similar way as PD-1^{24–25}; thus, we activated T cells using three classical methods, including CD3 and CD28, PMA and ionomycin, or PHA. The results revealed that both mRNA and protein levels of the PD-1^{IR2} and PD-1 were elevated after Jurkat cells activation, while PD-1 was relatively highly expressed compared with PD-1^{IR2} (figure 1E–J and online supplemental figure 1G). Furthermore, the temporal dynamics of *PDCD1*^{IR2} in Jurkat cells showed that *PDCD1*^{IR2} levels peaked on day 2 and modestly declined after day 3

(online supplemental figure 1K), suggesting that PD-1^{IR2} is a T cell activated expression protein.

We further found that *PDCD1*^{IR2} was expressed in both CD4⁺ and CD8⁺ T cells, but the level of *PDCD1*^{IR2} was much higher in CD8⁺ T cells compared with CD4⁺ T cells based on a public RNA-seq database²⁶ (figure 1K). Moreover, the expression of *PDCD1*^{IR2} was correlated with *PDCD1* (figure 1L). Analysis of CD8⁺ subsets of this database showed an increase of *PDCD1*^{IR2} in central memory T cells, effector memory T cells of type 1 and PD-1⁺CD39⁺ T cells compared with naive T cells (figure 1M), which were partially consistent with the expression of *PDCD1* in CD8⁺ subsets (figure 1N). Meanwhile, we analyzed *PDCD1*^{IR2} expression in the CD4⁺ subsets and found a notable increase in Follicular helper T cells (Tfh) compared with naive T cells (figure 1O), which was partially similar to the expression of *PDCD1* in CD4⁺ subsets (figure 1P), suggesting that PD-1^{IR2} potentially regulates T cell function. In addition, we found that *PDCD1*^{IR2} was increased in patients with cutaneous T-cell lymphoma compared with healthy individuals and its expression level was highly associated with tumor stage²⁷ (figure 1Q). To further investigate the expression of *PDCD1*^{IR2} and *PDCD1* in T cells, we analyzed RNA-sequencing of T cells from 364 patient samples across 10 different solid tumor types based on a public database,²⁸ which revealed that *PDCD1*^{IR2} and *PDCD1* were expressed in all of these tumor types (online supplemental figure 1L). We further isolated TILs from clinical lung cancer samples and found no difference between *PDCD1*^{IR2} and *PDCD1* expression (online supplemental figure 1M), which may be due to the small number of samples. Overall, these data reveal that PD-1^{IR2} is a new isoform of PD-1 and expresses in multiple T lymphocyte subsets or TILs from patient samples.

To identify the possible factors that regulate the generation of PD-1^{IR2}, we integrated literature and found that hnRNPLL is involved in both IR²⁹ and AS of CD45,³⁰ so we focused on the potential effect of hnRNPLL on IR of *PDCD1*. Endogenous hnRNPLL were knocked down by two independent short hairpin RNAs (shRNAs) in Jurkat cells (figure 1R), and qRT-PCR assays showed that knockdown (KD) of hnRNPLL reduced mRNA levels of *PDCD1*^{IR2} (figure 1S). In contrast, overexpression (OE) of hnRNPLL increased mRNA levels of *PDCD1*^{IR2} (figure 1T–V). We further investigated whether hnRNPLL binds to the *PDCD1* pre-mRNA and performed RNA immunoprecipitation (RIP) in Jurkat cells. The qRT-PCR assay showed that the pre-mRNA of *PDCD1*^{IR2} was higher enriched on hnRNPLL compared with IgG control (figure 1W). Collectively, these data suggest that hnRNPLL indeed binds to *PDCD1* pre-mRNA and regulates the generation of *PDCD1*^{IR2}.

PD-1^{IR2} inhibits the function of T cells in vitro

We next sought to evaluate the potential role of PD-1^{IR2} on the T cells and used two shRNAs targeting the second intron sequences of PD-1^{IR2} to knock down endogenous PD-1^{IR2} in Jurkat cells. The mRNA level of *PDCD1*^{IR2} was

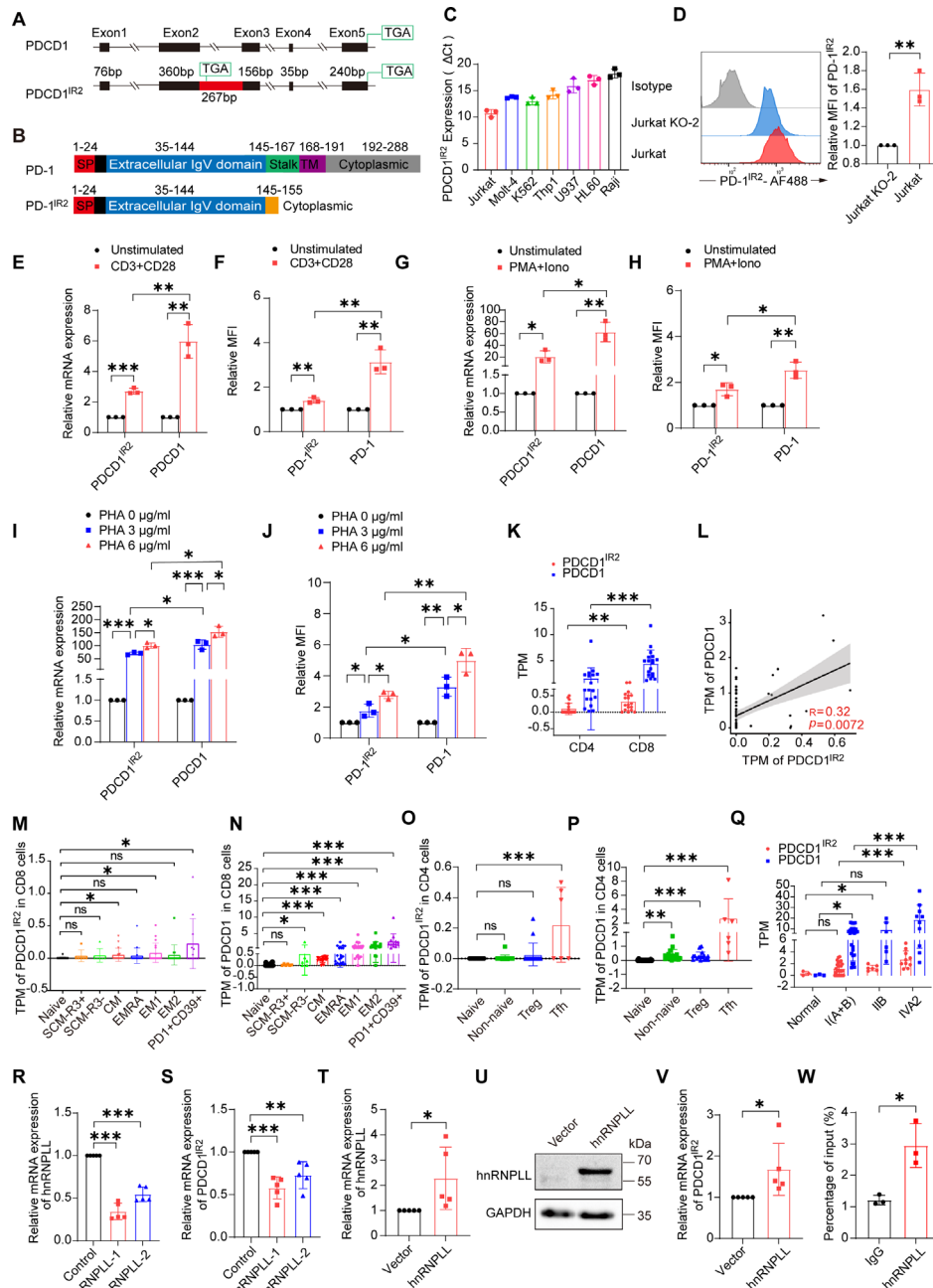


Figure 1 The identification and regulation of PD-1^{IR2}. (A, B) The schematic diagram for gene structure of *PDCD1* and *PDCD1^{IR2}* (A) and protein structure of PD-1 and PD-1^{IR2} (B). (C) qRT-PCR analysis for *PDCD1^{IR2}* in various human leukemia cell lines with PD-1^{IR2} specific primers (n=3). (D) Fluorescence-Activated Cell Sorting (FACS) analysis for PD-1^{IR2} protein level by PD-1^{IR2} specific monoclonal antibody in Phytohemagglutinin (PHA)-stimulated KO-2 Jurkat and Jurkat cells, with representative FACS images on the left and quantified results as the Mean fluorescence intensity (MFI) on the right (n=3). PHA: 5 μg/mL. (E-J) qRT-PCR analysis for mRNA levels of *PDCD1^{IR2}* and *PDCD1* (E, G and I), and FACS analysis for protein levels of PD-1^{IR2} and PD-1 (F, H and J) quantified as the MFI. Jurkat cells were stimulated with 5 μg/mL anti-CD3/CD28, 50 ng/mL Phorbol 12- myristate 13-acetate (PMA) and 1 μM Ionomycin, and 5 μg/mL PHA, respectively (n=3). (K-P) Analysis of RNA-seq data of healthy donors from public databases (GSE179613). (K) RNA-seq-derived transcripts per million (TPM) values of *PDCD1* and *PDCD1^{IR2}* in CD4⁺ and CD8⁺ T cells of PBMC. (L) The TPM of *PDCD1^{IR2}* was correlated with *PDCD1*. (M-N) Analysis for TPM of *PDCD1^{IR2}* and *PDCD1* in CD8⁺ subsets of this database. (O-P) Analysis for TPM of *PDCD1^{IR2}* and *PDCD1* in CD4⁺ subsets of this database. (Q) Analysis of RNA-seq data showed TPM values of *PDCD1* and *PDCD1^{IR2}* in patients with cutaneous T-cell lymphoma (CTCL) and healthy individuals (GSE113113). (R) qRT-PCR analysis for *hnRNPLL* in Jurkat cells transfected with the indicated shRNAs (n=5). (S) qRT-PCR analysis for *PDCD1^{IR2}* with *hnRNPLL* KD in Jurkat cells (n=5). (T-U) qRT-PCR and immunoblot analysis for mRNA (T) and protein level (U) of *hnRNPLL* in Jurkat cells transfected with the indicated plasmids (T, n=5). (V) qRT-PCR analysis for *PDCD1^{IR2}* with *hnRNPLL* OE in Jurkat cells (n=5). (W) qRT-PCR analysis for enrichment of pre-mRNA of *PDCD1^{IR2}* in Jurkat cells (n=3). Data represent the mean±SD or SEM. *p<0.05, **p<0.01, ***p<0.001. PBMC, peripheral blood mononuclear cells; PD-1, programmed cell death 1; qRT-PCR, quantitative RT-PCR; RT-PCR, reverse transcription-PCR.

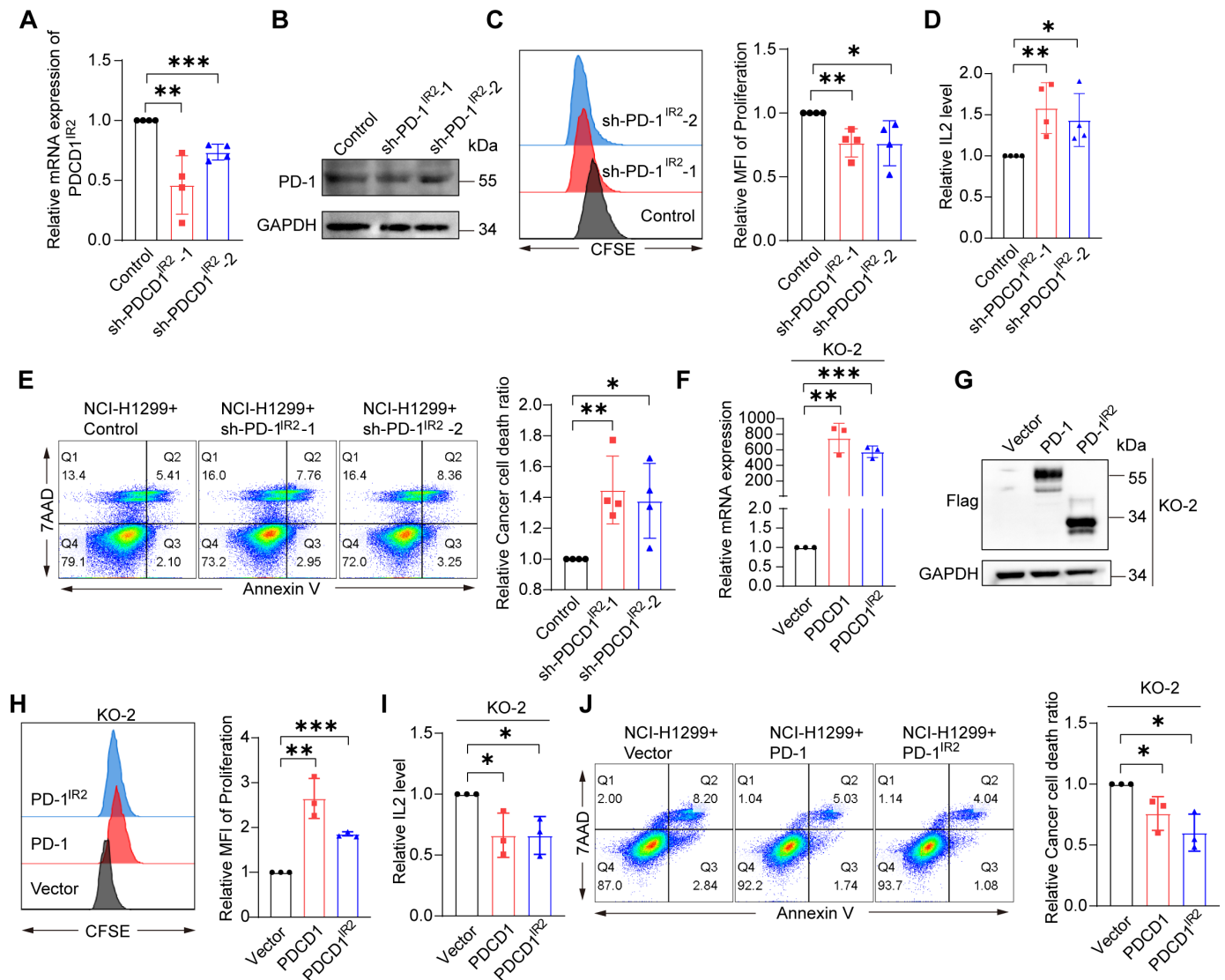


Figure 2 PD-1^{IR2} negatively regulates the immune function of T cells. (A) qRT-PCR analysis for mRNA level of *PDCD1*^{IR2} in Jurkat cells transfected with the indicated shRNAs (n=4). (B) Immunoblot analysis for protein level of PD-1 with *PDCD1*^{IR2} KD in Jurkat cells. (C) Carboxyfluorescein Succinimidyl Ester (CFSE) assay assessing the relative proliferation of Jurkat cells with *PDCD1*^{IR2} KD, representative FACS (left) and quantitation as the MFI (right) (n=4). (D) Quantification of IL-2 level in Jurkat cells with *PDCD1*^{IR2} KD (n=4). (E) Tumor cell killing of Jurkat cells with *PDCD1*^{IR2} KD against NCI-H1299 cells. The representative images (left) and the quantified ratio (right) of dead tumor cells measured by Annexin-V and 7-Aminoactinomycin D (7-AAD) staining (n=4). (F–G) qRT-PCR and Immunoblot analysis for mRNA (F) and protein levels (G) of PD-1 and PD-1^{IR2} in KO-2 Jurkat cells transfected with the indicated plasmids (F, n=3). (H) CFSE assay assessing the relative proliferation of KO-2 Jurkat cells with OE of *PDCD1* or *PDCD1*^{IR2}. Representative FACS (left) and quantitation as the MFI (right) (n=3). (I) Quantification of IL-2 level in KO-2 Jurkat cells with OE of *PDCD1* or *PDCD1*^{IR2} (n=3). (J) Tumor cell killing of KO-2 Jurkat cells with OE of *PDCD1* or *PDCD1*^{IR2} against NCI-H1299 cells. The representative images (left) and the quantified ratio (right) of dead tumor cells measured by Annexin-V and 7AAD staining (n=3). Data presented as means±SD or SEM. *p<0.05, **p<0.01, ***p<0.001. IL, interleukin; KD, knockdown; OE, overexpression; PBMC, peripheral blood mononuclear cells; PD-1, programmed cell death 1; qRT-PCR, quantitative RT-PCR; RT-PCR, reverse transcription-PCR; shRNAs, short hairpin RNAs.

correspondingly reduced in PD-1^{IR2}-KD cells compared with control (figure 2A), but PD-1 protein level was not affected (figure 2B). PD-1^{IR2} KD enhanced cell proliferation and IL-2 production in Jurkat cells (figure 2C,D), and exhibited an increased killing ability against NCI-H1299 tumor cells (figure 2E and online supplemental figure 2A). In contrast, we overexpressed *PDCD1* and *PDCD1*^{IR2} in two PD-1 KO cell lines, respectively (figure 2F and G and online supplemental figure 2B,C), and found that

PD-1^{IR2} OE attenuated cell proliferation and cytokine production, and the ability of killing NCI-H1299 tumor cells compared with control. The similar results were observed for PD-1 OE (figure 2H–J and online supplemental figure 2D–F), consistent with previous study that PD-1 plays a crucial role in suppressing the activation of T cells.^{31 32} Overall, these data demonstrate that PD-1^{IR2} is a potential IC that negatively modulates the immune response of T cells.

Given that PD-L1 exists not only on the membrane but also in the cytoplasm of CD8⁺ T cells to exert function,³³ while the IgV domain (K78, I126, and E136) responsible for PD-1 binding to PD-L1 is retained in PD-1^{IR2} (figure 1B). Therefore, we hypothesized that PD-1^{IR2} may engage with cytoplasmic PD-L1 to exert function. To verify this, we employed the OE strategy of *PDCD1^{IR2}* and *PDCD1LG1* in both KO-1 and KO-2 cells. The results indicated that simultaneous OE of *PDCD1^{IR2}* and *PDCD1LG1* suppressed cell proliferation and IL-2 production compared with OE of *PDCD1^{IR2}* alone (online supplemental figure 2G–J), which revealed that PD-1^{IR2} can exert immunosuppressive function at least to some extent by binding with PD-L1.

Antitumor response is impaired in PD-1^{IR2} knock-in mice

Although a murine *Pdcd1* isoform similar to *PDCD1^{IR2}* is absent in mouse, murine PD-L1 can interact with human PD-1 to inhibit the function of T cells, due to the similar molecular structure to human PD-L1.³⁴ To further study the physiological function of PD-1^{IR2}, *PDCD1^{IR2} flox/flox* mice were generated and crossed with Cd4^{cre} mice to specifically conditional knock-in (CKI) *PDCD1^{IR2}* in T cells (*PDCD1^{IR2} CKI (PDCD1^{IR2} CKI)* mice) (online supplemental figure 3A–C). *PDCD1^{IR2} CKI* did not affect the development, peripheral homeostasis of T cells and the population of memory T cells (online supplemental figure 3D–K). *PDCD1^{IR2} CKI* CD8⁺ T cells showed decreased cytokines compared with the WT cells stimulated using anti-CD3 and anti-CD28 antibodies, including GzmB and interferon (IFN)- γ (online supplemental figure 4A,B). However, there was no change in proliferation and cell death between the two groups (online supplemental figure 4C,D), indicating that PD-1^{IR2} partially impairs T cell function. To further gain insights into the downstream signaling pathway, we performed RNA-sequencing (RNA-seq) in WT and *PDCD1^{IR2} CKI* CD8⁺ T cells. Differentially expressed genes (DEGs) analysis showed that 333 genes were significantly upregulated, whereas 911 genes were downregulated in *PDCD1^{IR2} CKI* CD8⁺ T cells (online supplemental figure 4E). Gene ontology analysis showed that DEGs were mostly enriched in immunity-related pathways, such as cytokine-mediated signaling pathway, leukocyte-mediated immunity and activation of the immune response (online supplemental figure 4F), indicating that *PDCD1^{IR2}* regulates immune response. In the leukocyte-mediated immunity pathway, we observed downregulation of *Gzmb*, *Ifng*, *Tbx21*, and *Il2rb* gene expression in *PDCD1^{IR2} CKI* CD8⁺ T cells (online supplemental figure 4G), further revealing that PD-1^{IR2} can partially impair T cell function.

We next used MC38 colorectal carcinoma models to explore the function of PD-1^{IR2} in tumor (figure 3A). *PDCD1^{IR2} CKI* mice showed faster tumor growth than WT mice, indicated by an increase in tumor volume and tumor weight (figure 3B–D). Furthermore, we observed a comparable proportion of CD44 in tumor-infiltrating CD8⁺ T cells in *PDCD1^{IR2} CKI* and WT mice, indicating the

similar antigen experience (figure 3E). The percentages of CD4⁺ T cells and CD8⁺ T cells and Treg cells in the TIL were not affected by *PDCD1^{IR2} CKI* (figure 3F and G). In addition, we did not observe a significant change in Ki-67 expression in tumor-infiltrating CD8⁺ T cells (figure 3H). However, GzmB and IFN- γ in tumor-infiltrating CD8⁺ T cells were attenuated compared with WT mice (figure 3I and J), suggesting impaired cytotoxic ability. We analyzed the immune landscape in mouse spleen and found that these cells were not affected (online supplemental figure 5A–E). Subsequently, we transplanted MC38 cancer cells into WT and *PDCD1^{IR2} CKI* mice and treated them with anti-PD-L1 or IgG, which revealed that treatment with anti-PD-L1 antibody significantly retarded the tumor growth compared with IgG treatment in WT mice, whereas *PDCD1^{IR2} CKI* mice showed resistance to anti-PD-L1 therapy and repressed function of CD8⁺ T cells (figure 3K–N). Indeed, we still observed a certain effect of anti-PD-L1 treatment on tumors in *PDCD1^{IR2} CKI* mice, as shown by the reduced tumor volume and weight as well as increased production of GzmB (figure 3K–N, CKI+anti-PD-L1 vs CKI+IgG). However, the tumor volume in *PDCD1^{IR2} CKI* mice remained larger than that in WT mice (figure 3K, CKI+anti-PD-L1 vs WT+anti-PD-L1), indicating that PD-1^{IR2} can still exert immune suppression after anti-PD-L1 treatment. However, after anti-PD-L1 treatment, the tumor weight in the CKI group tended to be larger than that in WT group with no statistical difference (figure 3M). The population of Treg cells decreased in both WT and *PDCD1^{IR2} CKI* mice (figure 3O), consistent with a previous report in which checkpoint blockade therapy was used.³⁵ Together, these data demonstrate that antitumor effects are impaired in *PDCD1^{IR2} CKI* mice, which show resistance to IC blockade.

PD-1^{IR2} effectively promotes tumor progression by reducing function of intratumoral CD8⁺ T cells

To further confirm the inhibitory role of PD-1^{IR2} in anti-tumor immunity, we challenged NCI-H1299 tumor cells in humanized PBMC (huPBMC)-NOG (NOD.Cg-Prkdc-sid1L2rgtm1Sug/JicCr1) mice, in which human PBMCs overexpressed PD-1^{IR2} (figure 4A). PD-1^{IR2} huPBMC-NOG mice had an impaired ability to restrain tumor growth compared with the control, supported by an increase in tumor volume and weight (figure 4B–D). Consistent with data from *PDCD1^{IR2} CKI* mice, CD44 activation in tumor-infiltrating CD8⁺ T cells showed no significant differences compared with control mice (figure 4E). In addition, we did not observe significant changes in the frequency of CD4⁺ T cells and CD8⁺ T cells in huPBMC-NOG mice (figure 4F). Ki-67 expression was not affected in tumor-infiltrating CD8⁺ T cells (figure 4G). Immune function of CD8⁺ T cells was partially impaired in PD-1^{IR2} huPBMC-NOG mice indicated by decreased cytokine production, including GzmB and IFN- γ (figure 4H). Consistent with our above findings, these indicators were not changed in mouse spleen compared with control (figure 4I–L), suggesting that tumor antigen presentation

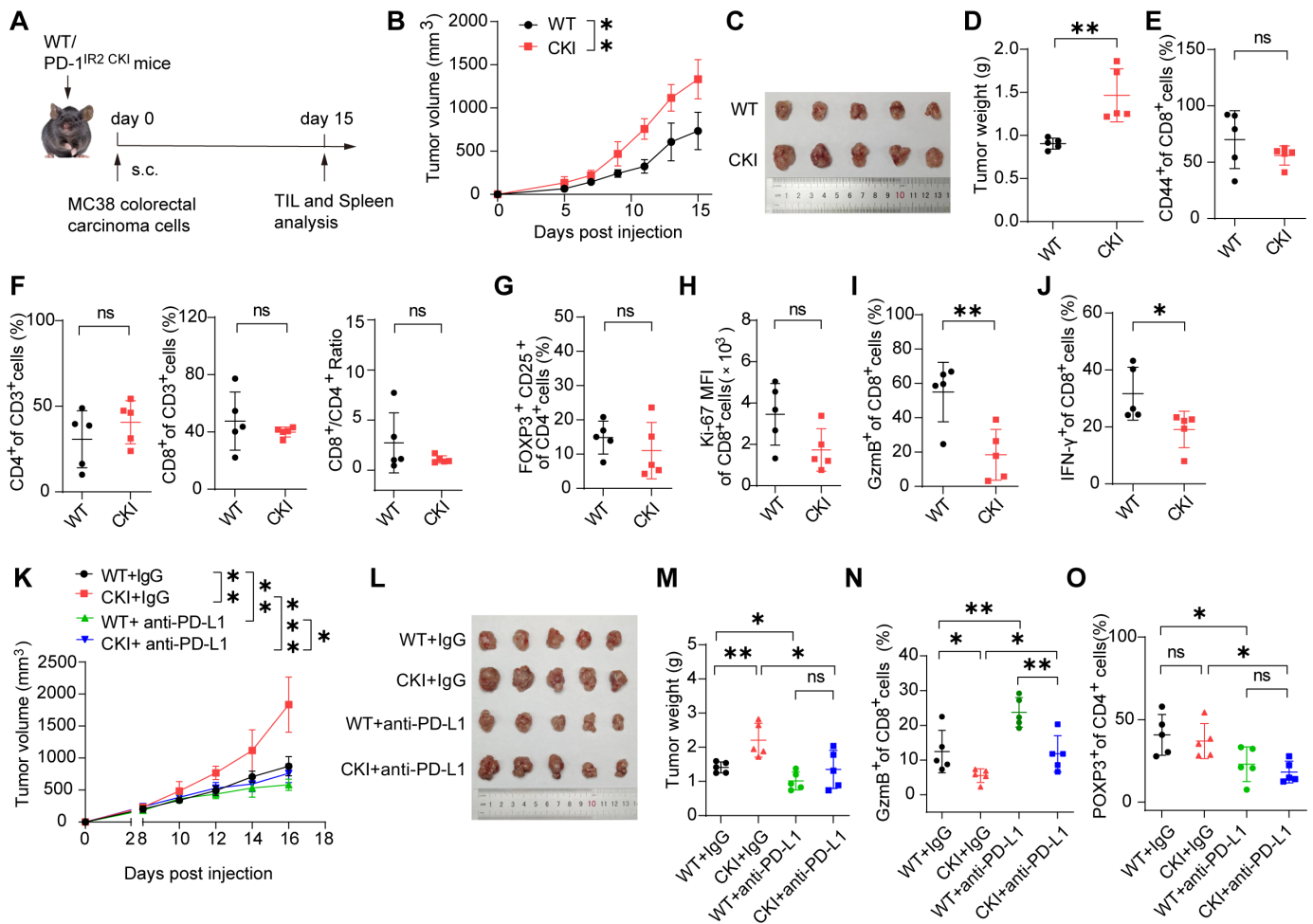


Figure 3 Antitumor response is impaired in PD-1^{IR2} knock-in mice. (A) A schematic plan for WT or *PDCD1*^{IR2 CKI} mice bearing subcutaneous MC38 tumors. (B–D) Subcutaneous MC38 tumor growth curve in WT and *PDCD1*^{IR2 CKI} mice; statistical analysis was performed using two-sided t-tests for the tumor volume at the end point (B); images of MC38 tumors at the end point (C), and tumor weight of MC38 tumors (D). *n*=5 mice per group. (E) Flow cytometry analysis showing the percentage of CD44⁺ in tumor-infiltrating CD8⁺ T cells derived from WT or *PDCD1*^{IR2 CKI} mice. (F–G) Flow cytometry analysis showing the percentage of CD4⁺, CD8⁺, quantified ratio of CD8⁺ to CD4⁺ (F) in CD3⁺ T cells, and Foxp3⁺ (G) in CD4⁺ T cells in subcutaneous MC38 tumors derived from WT or *PDCD1*^{IR2 CKI} mice. (H) Ki-67 MFI in tumor-infiltrating CD8⁺ T cells. (I–J) The percentages of GzmB⁺ and IFN-γ⁺ in tumor-infiltrating CD8⁺ T cells. (K–M) Subcutaneous MC38 tumor growth curves in WT and *PDCD1*^{IR2 CKI} mice with indicated treatments, statistical analysis was performed using two-sided t-tests for the tumor volume at the end point (K); images of MC38 tumors at the end point (L), and tumor weight of MC38 tumors (M). *n*=5 mice per group. (N–O) Flow cytometry analysis showing the percentage of GzmB⁺ in tumor-infiltrating CD8⁺ T cells (N), and Foxp3⁺ in CD4⁺ T cells (O) derived from WT or *PDCD1*^{IR2 CKI} mice after indicated treatments. Data represent the mean±SD. **p*<0.05, ***p*<0.01, ****p*<0.001. CKI, conditional knock-in; IFN, interleukin; PD-1, programmed cell death 1; WT, wild type.

is limited to the tumor microenvironment. In conclusion, these results highlight that PD-1^{IR2} is a potentially novel IC that negatively regulates antitumor immunity in vivo.

DISCUSSION

IC inhibitor (ICI) therapy primarily targets CTLA-4, PD-1 and its ligand PD-L1.³⁶ These ICIs have achieved significant efficacy in some patients. However, a large population does not respond or develop resistance.^{37,38} AS is a key mechanism for regulating gene expression and maintaining protein diversity, taking place in about 95% of human genes.³⁹ Immune cells undergo extensive AS during development and differentiation, generating

multiple transcripts to compensate for the limited genes involved in immune responses.^{40,41} AS is involved in the regulation of ICs; the existence of the isoforms generated by AS may contribute to the low response of ICIs therapy.

AS plays an important role in regulating the expression of IC molecules; several PD-1 isoforms from AS have been reported, such as Δ42PD-1 and PD-1Δ ex3. Δ42PD-1 contains a 42-nucleotide in-frame deletion located at exon 2 domain, which amplifies the generation of antigen-specific CD8⁺ T cell immunity when used in a DNA vaccine.¹¹ Hence, Δ42PD-1 enhance antigen-specific immunity and protect mice against pathogenic viral challenge and tumor growth.¹¹ In another study, Δ42PD1 T

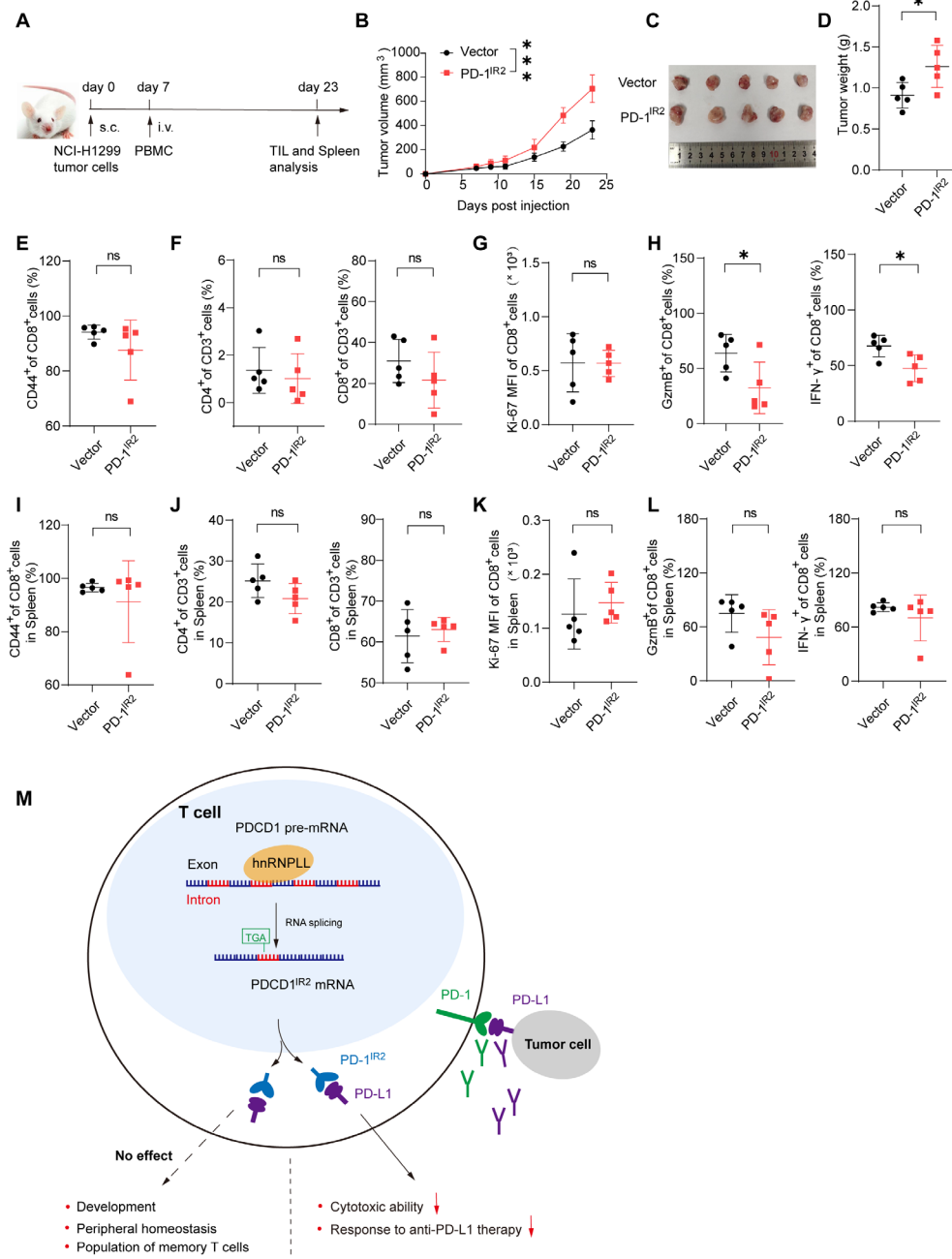


Figure 4 PD-1^{IR2} effectively promotes tumor progression by reducing function of intratumoral CD8⁺ T cells. (A) A schematic plan for control or PD-1^{IR2} huPBMC-NOG mice bearing subcutaneous NCI-H1299 tumors. (B–D) Subcutaneous NCI-H1299 tumor growth curve in control and PD-1^{IR2} huPBMC-NOG mice; statistical analysis was performed using two-sided t-tests for the tumor volume at the end point (B); images of NCI-H1299 tumors at the end point (C), and tumor weight of NCI-H1299 tumors (D). n=5 mice per group. (E) Flow cytometry analysis showing the percentage of CD44⁺ in tumor-infiltrating CD8⁺ T cells derived from control and PD-1^{IR2} huPBMC-NOG mice. (F) Flow cytometry analysis showing the percentage of CD4⁺, CD8⁺ in CD3⁺ T cells in subcutaneous NCI-H1299 tumors derived from control and PD-1^{IR2} huPBMC-NOG mice. (G) Ki-67 MFI in tumor-infiltrating CD8⁺ T cells. (H) The percentage of GzmB⁺ and IFN- γ ⁺ in tumor-infiltrating CD8⁺ T cells. (I–L) Immune landscape of mouse spleen in control and PD-1^{IR2} huPBMC-NOG mice subcutaneously implanted with NCI-H1299 cells. Spleen T cells were isolated and analyzed on day 23, n=5 mice per group. (I) Flow cytometry analysis showing the percentage of CD44⁺ in spleen CD8⁺ T cells derived from control and PD-1^{IR2} huPBMC-NOG mice. (J) The percentage of CD4⁺ and CD8⁺ in spleen CD3⁺ T cells. (K) Ki-67 MFI in spleen CD8⁺ T cells. (L) The percentages of GzmB⁺ and IFN- γ ⁺ in spleen CD8⁺ T cells. (M) Proposed model for the PD-1^{IR2} promoting tumor progression. PD-1^{IR2} is expressed in T lymphocytes at transcription and protein levels, which is regulated by RNA-binding protein hnRNPLL. PD-1^{IR2} did not affect the development, peripheral homeostasis of T cells and the population of memory T cells without tumor infiltration. When challenged with tumor, PD-1^{IR2}⁺ CD8⁺ T cells showed decreased cytotoxic ability and resistance to anti-PD-L1 therapy. Data represent the mean \pm SD. *p<0.05, **p<0.01, ***p<0.001. ns, not significant. huPBMC, humanized PBMC; IFN, interferon; PBMC, peripheral blood mononuclear cells; PD-1, programmed cell death 1; PD-L1, PD-1 ligand 1; TIL, tumor infiltrating lymphocyte.

cells were tumor-infiltrating and correlated positively with HCC severity; moreover, $\Delta 42$ PD1 were more exhausted than PD-1⁺ T cells by single T cell and functional analysis.¹² These two studies suggest that the molecular function of $\Delta 42$ PD-1 is inclusive. The PD-1 Δ ex3, which lacks exon 3, is presumably secreted as a soluble form; it could functionally block the membrane-bound PD-1 and is elevated in patients with rheumatoid arthritis.⁴² In another study, an increase in PD-1 Δ ex3 during erlotinib treatment was associated with prolonged progression-free and overall survival in patients with non-small cell lung cancer.¹⁴ Interestingly, PD-1^{Δ28} serves as a new intracellular IC, which promotes tumor progression in mice and mediates resistance to immunotherapy.¹⁸ These studies reveal that the function of PD-1 isoforms may be identical, or antagonistic with PD-1.

In our study, we identified a novel isoform PD-1^{IR2}, which expresses in a variety of human leukemia cell lines and clinical tumor biopsies. We elucidated that hnRNPLL mediates the generation of *PDCDI*^{IR2}. PD-1^{IR2} negatively regulates the immune function of CD8⁺ T cells, including proliferation, cytokine production, and tumor cell killing in vitro. We further explored the function of PD-1^{IR2} using a mouse model in vivo. PD-1^{IR2} CD8⁺ T cells show impaired antitumor function, including a reduced production of GzmB and IFN- γ , which consequently promote tumor evasion in *PDCDI*^{IR2 CKI} mice. The same results have been observed in PBMC-engrafted humanized NOG mouse model. *PDCDI*^{IR2 CKI} mice exhibit resistance to anti-PD-L1 therapy compared with WT mice, indicated by increased tumor volume and reduced GzmB secretion. In summary, we demonstrate that PD-1^{IR2} mediates tumor immune evasion and resistance to anti-PD-L1 antibody (figure 4M). These data suggest that PD-1^{IR2} is a potential IC and may mediate the resistance in immunotherapy for patients with cancer.

Despite structural changes due to premature termination codons, PD-1^{IR2} retains the PD-L1 binding domain which was encoded by exon 2. In our study, we demonstrated that PD-1^{IR2} can bind to PD-L1 ligand to exert its biological function at least to some extent. However, PD-1^{IR2} contains a short (10 amino acids) and undefined cytoplasmic tail, suggesting that PD-1^{IR2} may not initiate intracellular signaling directly. When PD-1^{IR2} binds to PD-L1, it may not exert function through the traditional signaling pathways, and still requires further exploration to understand how it transmits inhibitory signals. Interestingly, intracellular signal pathway of PD-1 can be blocked via enforced phosphatase recruitment⁴³; thus, it is imperative to explore whether the signals of PD-1^{IR2} can be similarly disrupted in the future. Moreover, the isoform $\Delta 42$ PD-1 promotes cytokine secretion by binding to TLR4 but not PD-L1/PD-L2 ligands in $\gamma\delta$ -T cells and dendritic cells^{44 45}; this implies that PD-1^{IR2} may also regulate immune function through other ligands or signaling pathways. One study has reported that human PD-1 is more inhibitory than mouse PD-1^{IR2}; therefore, comparing the effects of PD-1 and PD-1^{IR2} through mice

expressing human PD-1 is imperative to be explored in the future. However, experiments in vitro confirmed that PD-1^{IR2} exhibits inhibitory effects similar to those of PD-1 (figure 2C–E and H–J, and online supplemental figure 2D–F). We failed to identify PD-1^{IR2} in mouse, but it does not rule out the existence of other isoforms with similar function. Also, we observed that mice expressing PD-1^{IR2} mediate resistance to ICIs, but we did not validate this in the human patient cohort. PD-1 is expressed in the innate immune cells,^{47–50} which may mediate suppressive signals. It is still expected to explore whether PD-1^{IR2} plays a function in innate immune cells.

Author affiliations

¹Department of Microbiology and Immunology, Shanxi Medical University, Taiyuan, Shanxi, China

²Shanxi Academy of Advanced Research and Innovation, Taiyuan, Shanxi, China

³School of Life Sciences and Technology, Advanced Institute for Life and Health, Southeast University Zhongda Hospital, Nanjing, Jiangsu, China

⁴Medical College, Guizhou University, Guiyang, Guizhou, China

⁵School of Biomedical Engineering (Suzhou), Division of Life Sciences and Medicine, University of Science and Technology of China, Hefei, Anhui, China

⁶Medical School of Nanjing University, Nanjing, Jiangsu, China

⁷The Key Laboratory of Medical Molecular Cell Biology of Shanxi Province, Institutes of Biomedical Sciences, Shanxi University, Taiyuan, Shanxi, China

⁸Department of oncology, The Key Laboratory of Advanced Interdisciplinary Studies, First Affiliated Hospital of Guangzhou Medical University State Key Laboratory of Respiratory Disease, Guangzhou, Guangdong, China

⁹The Second Affiliated Hospital, Zhejiang University School of Medicine, Hangzhou, Zhejiang, China

¹⁰School of Medicine, Southeast University, Nanjing, Jiangsu, China

¹¹Center for Immunology and Hematology, Department of Biotherapy and Cancer Center, State Key Laboratory of Biotherapy, West China Hospital, Sichuan University, Chengdu, China

Acknowledgements We thank Yibi Zhang for helping us perform research. Zhenye Pu for providing us with clinical samples. Mang Shang for helping us review the paper and providing funding support.

Contributors SG, HZ, HH, and YG designed research, wrote and reviewed the paper. SG is the guarantor of the work. HZ, TL, and XiaodongW collected and analyzed the data. HZ, TL, XiaodongW, XZhu, CH, FG, CZ, and FY performed research. SC and LD provided bioinformatics support and analyzed data. XZhao reviewed the paper. XuetongW designed research and gave advice.

Funding This work was supported by National Key 373 R&D Program of China (2022YFC3401000); by the National Natural Science Foundation of China (82430094, 8205029, 82150114, 8205002, 32230036 and 82403276); by grants from the Natural Science Foundation of Jiangsu Province (BK20240271).

Competing interests No, there are no competing interests.

Patient consent for publication Not applicable.

Ethics approval Not applicable.

Provenance and peer review Not commissioned; externally peer reviewed.

Data availability statement Data are available in a public, open access repository.

Supplemental material This content has been supplied by the author(s). It has not been vetted by BMJ Publishing Group Limited (BMJ) and may not have been peer-reviewed. Any opinions or recommendations discussed are solely those of the author(s) and are not endorsed by BMJ. BMJ disclaims all liability and responsibility arising from any reliance placed on the content. Where the content includes any translated material, BMJ does not warrant the accuracy and reliability of the translations (including but not limited to local regulations, clinical guidelines, terminology, drug names and drug dosages), and is not responsible for any error and/or omissions arising from translation and adaptation or otherwise.

Open access This is an open access article distributed in accordance with the Creative Commons Attribution Non Commercial (CC BY-NC 4.0) license, which permits others to distribute, remix, adapt, build upon this work non-commercially,

and license their derivative works on different terms, provided the original work is properly cited, appropriate credit is given, any changes made indicated, and the use is non-commercial. See <http://creativecommons.org/licenses/by-nc/4.0/>.

ORCID iDs

Haojing Zang <http://orcid.org/0009-0000-5545-3603>

Yinmin Gu <http://orcid.org/0000-0001-9825-5447>

Shan Gao <http://orcid.org/0000-0003-0262-4549>

REFERENCES

- Haanen JBAG, Robert C. Immune Checkpoint Inhibitors. *Prog Tumor Res* 2015;42:55–66.
- Postow MA, Callahan MK, Wolchok JD. Immune Checkpoint Blockade in Cancer Therapy. *J Clin Oncol* 2015;33:1974–82.
- Okazaki T, Honjo T. PD-1 and PD-1 ligands: from discovery to clinical application. *Int Immunol* 2007;19:813–24.
- Latcham Y, Wood CR, Chernova T, et al. PD-L2 is a second ligand for PD-1 and inhibits T cell activation. *Nat Immunol* 2001;2:261–8.
- Freeman GJ, Long AJ, Iwai Y, et al. Engagement of the PD-1 immunoinhibitory receptor by a novel B7 family member leads to negative regulation of lymphocyte activation. *J Exp Med* 2000;192:1027–34.
- Sharma P, Allison JP. The future of immune checkpoint therapy. *Science* 2015;348:56–61.
- Marasco LE, Kornblith AR. The physiology of alternative splicing. *Nat Rev Mol Cell Biol* 2023;24:242–54.
- Mourich DV, Oda SK, Schnell FJ, et al. Alternative splice forms of CTLA-4 induced by antisense mediated splice-switching influences autoimmune diabetes susceptibility in NOD mice. *Nucleic Acid Ther* 2014;24:114–26.
- Ichinose K, Zhang Z, Koga T, et al. Brief report: increased expression of a short splice variant of CTLA-4 exacerbates lupus in MRL/lpr mice. *Arthritis Rheum* 2013;65:764–9.
- Gu M, Kakoulidou M, Giscoombe R, et al. Identification of CTLA-4 isoforms produced by alternative splicing and their association with myasthenia gravis. *Clin Immunol* 2008;128:374–81.
- Zhou J, Cheung AK, Liu H, et al. T cell immunity by a novel PD1 isoform-based fusion DNA vaccine. *Mol Ther* 2013;21:1445–55.
- Tan Z, Chiu MS, Yang X, et al. Isoformic PD-1-mediated immunosuppression underlies resistance to PD-1 blockade in hepatocellular carcinoma patients. *Gut* 2023;72:1568–80.
- Sun J, Bai J, Jiang T, et al. Modulation of PDCD1 exon 3 splicing. *RNA Biol* 2019;16:1794–805.
- Sorensen SF, Demuth C, Weber B, et al. Increase in soluble PD-1 is associated with prolonged survival in patients with advanced EGFR-mutated non-small cell lung cancer treated with erlotinib. *Lung Cancer (Auckl)* 2016;100:77–84.
- Wang C, Weng M, Xia S, et al. Distinct roles of programmed death ligand 1 alternative splicing isoforms in colorectal cancer. *Cancer Sci* 2021;112:178–93.
- Qu S, Jiao Z, Lu G, et al. PD-L1 lncRNA splice isoform promotes lung adenocarcinoma progression via enhancing c-Myc activity. *Genome Biol* 2021;22:104.
- Nielsen C, Ohm-Laursen L, Barington T, et al. Alternative splice variants of the human PD-1 gene. *Cell Immunol* 2005;235:109–16.
- Wang X, Liu T, Li Y, et al. A splicing isoform of PD-1 promotes tumor progression as a potential immune checkpoint. *Nat Commun* 2024;15:9114.
- Galante PAF, Sakabe NJ, Kirschbaum-Slager N, et al. Detection and evaluation of intron retention events in the human transcriptome. *RNA* 2004;10:757–65.
- Wang ET, Sandberg R, Luo S, et al. Alternative isoform regulation in human tissue transcriptomes. *Nature New Biol* 2008;456:470–6.
- Barash Y, Calarco JA, Gao W, et al. Deciphering the splicing code. *Nature New Biol* 2010;465:53–9.
- Nilsen TW, Graveley BR. Expansion of the eukaryotic proteome by alternative splicing. *Nature New Biol* 2010;463:457–63.
- Ni T, Yang W, Han M, et al. Global intron retention mediated gene regulation during CD4+ T cell activation. *Nucleic Acids Res* 2016;44:6817–29.
- Ishida Y, Agata Y, Shibahara K, et al. Induced expression of PD-1, a novel member of the immunoglobulin gene superfamily, upon programmed cell death. *EMBO J* 1992;11:3887–95.
- Agata Y, Kawasaki A, Nishimura H, et al. Expression of the PD-1 antigen on the surface of stimulated mouse T and B lymphocytes. *Int Immunol* 1996;8:765–72.
- Giles JR, Manne S, Freilich E, et al. Human epigenetic and transcriptional T cell differentiation atlas for identifying functional T cell-specific enhancers. *Immunity* 2022;55:557–74.
- Querfeld C, Leung S, Myskowski PL, et al. Primary T Cells from Cutaneous T-cell Lymphoma Skin Explants Display an Exhausted Immune Checkpoint Profile. *Cancer Immunol Res* 2018;6:900–9.
- Combes AJ, Samad B, Tsui J, et al. Discovering dominant tumor immune archetypes in a pan-cancer census. *Cell* 2022;185:184–203.
- Monteuuis G, Wong JLL, Bailey CG, et al. The changing paradigm of intron retention: regulation, ramifications and recipes. *Nucleic Acids Res* 2019;47:11497–513.
- Oberdoerffer S, Moita LF, Neems D, et al. Regulation of CD45 alternative splicing by heterogeneous ribonucleoprotein, hnRNPL. *Science* 2008;321:686–91.
- Nishimura H, Nose M, Hiai H, et al. Development of lupus-like autoimmune diseases by disruption of the PD-1 gene encoding an ITIM motif-carrying immunoreceptor. *Immunity* 1999;11:141–51.
- Liu J, Yuan Y, Chen W, et al. Immune-checkpoint proteins VISTA and PD-1 nonredundantly regulate murine T-cell responses. *Proc Natl Acad Sci USA* 2015;112:6682–7.
- Wang X, Lu L, Hong X, et al. Cell-intrinsic PD-L1 ablation sustains effector CD8+ T cell responses and promotes antitumor T cell therapy. *Cell Rep* 2024;43:113712.
- Magiera-Mularz K, Kocik J, Musielak B, et al. Human and mouse PD-L1: similar molecular structure, but different druggability profiles. *iScience* 2021;24:101960.
- Wei SC, Levine JH, Cogdill AP, et al. Distinct Cellular Mechanisms Underlie Anti-CTLA-4 and Anti-PD-1 Checkpoint Blockade. *Cell* 2017;170:1120–33.
- Xiao Q, Nobre A, Piñeiro P, et al. Genetic and Epigenetic Biomarkers of Immune Checkpoint Blockade Response. *J Clin Med* 2020;9:286.
- Champiat S, Derle L, Ammari S, et al. Hyperprogressive Disease Is a New Pattern of Progression in Cancer Patients Treated by Anti-PD-1/PD-L1. *Clin Cancer Res* 2017;23:1920–8.
- Pires da Silva I, Ahmed T, Reijers ILM, et al. Ipilimumab alone or ipilimumab plus anti-PD-1 therapy in patients with metastatic melanoma resistant to anti-PD-(L)1 monotherapy: a multicentre, retrospective, cohort study. *Lancet Oncol* 2021;22:836–47.
- Kjer-Hansen P, Weatheritt RJ. The function of alternative splicing in the proteome: rewiring protein interactomes to put old functions into new contexts. *Nat Struct Mol Biol* 2023;30:1844–56.
- Bechara R, Vagner S, Mariette X. Post-transcriptional checkpoints in autoimmunity. *Nat Rev Rheumatol* 2023;19:486–502.
- Martinez NM, Lynch KW. Control of alternative splicing in immune responses: many regulators, many predictions, much still to learn. *Immunol Rev* 2013;253:216–36.
- Wan B, Nie H, Liu A, et al. Aberrant Regulation of Synovial T Cell Activation by Soluble Costimulatory Molecules in Rheumatoid Arthritis. *The Journal of Immunology* 2006;177:8844–50.
- Fernandes RA, Su L, Nishiga Y, et al. Immune receptor inhibition through enforced phosphatase recruitment. *Nature New Biol* 2020;586:779–84.
- Cheung AKL, Kwok H-Y, Huang Y, et al. Gut-homing $\Delta 42PD1^*V\delta 2$ T cells promote innate mucosal damage via TLR4 during acute HIV type 1 infection. *Nat Microbiol* 2017;2:1389–402.
- Mo Y, Cheung AKL, Liu Y, et al. $\Delta 42PD1$ -TLR4 Augments $\gamma\delta$ -T Cell Activation of the Transitional Memory Subset of CD4⁺ T Cells. *iScience* 2020;23:101620.
- Masubuchi T, Chen L, Marcel N, et al. Functional differences between rodent and human PD-1 linked to evolutionary divergence. *Sci Immunol* 2025;10:eads6295.
- Huang X, Venet F, Wang YL, et al. PD-1 expression by macrophages plays a pathologic role in altering microbial clearance and the innate inflammatory response to sepsis. *Proc Natl Acad Sci U S A* 2009;106:6303–8.
- Yu Y, Tsang JCH, Wang C, et al. Single-cell RNA-seq identifies a PD-1hi ILC progenitor and defines its development pathway. *Nature New Biol* 2016;539:102–6.
- Shen L, Gao Y, Liu Y, et al. PD-1/PD-L pathway inhibits M.tb-specific CD4⁺ T-cell functions and phagocytosis of macrophages in active tuberculosis. *Sci Rep* 2016;6:38362.
- Pesce S, Greppi M, Tabellini G, et al. Identification of a subset of human natural killer cells expressing high levels of programmed death 1: A phenotypic and functional characterization. *J Allergy Clin Immunol* 2017;139:335–46.